Polymer Chemistry

ROYAL SOCIETY OF CHEMISTRY

PAPER

View Article Online
View Journal

Cite this: DOI: 10.1039/d6py00213g

Metal-free synthesis of terpene-derived polyester-*block*-polycarbonates and post-polymerization modification *via* thiol–ene click chemistry

Mikhailey D. S. Wheeler, Allison M. Clark, Andrew P. Kinsman, Megan L. Graham and Francesca M. Kerton *

Sustainable polymers are a large research focus due to depleting resources and increasing environmental pollution. Therefore, renewable feedstocks are being pursued as an alternative to fossil-derivatives for producing polymers. Here, we have prepared a series of polyester and polyester-*block*-polycarbonate copolymers *via* metal-free ring-opening copolymerizations (ROCOPs) of various terpene-derived cyclic anhydrides, epoxides [cyclohexene oxide (CHO) and propylene oxide (PO)], and carbon dioxide (CO_2) under neat (solvent-free) conditions. Cyclic anhydrides were prepared *via* microwave-assisted Diels Alder reactions between terpenes and maleic anhydride (up to 90% yield) with no purification required. The ROCOP catalyst system consisted of triphenylborane (BPh_3) with bis(triphenylphosphine)iminium chloride (PPNCl) and resulted in polymers with moderate molecular weights ($M_n \leq 13$ kDa), and dispersities ($1.05 \leq Đ \leq 1.75$). Thermal analysis resulted in a single glass transition temperature (1.5 °C $\leq T_g \leq$ 101 °C) indicating amorphous materials. $^{13}C\{^1H\}$ NMR spectroscopy revealed high stereoregularity with respect to substituent methyl groups and di-ester units and 2D DOSY NMR spectroscopy confirmed a single polymer chain was formed by sequential copolymerizations. Residual olefinic groups in these polymers were subjected to post-polymermization functionalization *via* photoinitiated thiol–ene (3-mercaptopropionic acid and butyl 3-mercaptopropionate) 'click' chemistry with 2,2-dimethoxy-2-phenylacetophenone as the photoinitiator. High degrees of functionalization (>99%), increased molecular weights ($M_n \leq 49$ kDa), and differing solubilities and hydrophilicities were observed. Thermal analysis further demonstrated the ability to tune polymer properties; modified polymers yielded high decomposition temperatures (≈300 °C) and dramatically different T_g than the non-functionalized precursors, and one modified polymer displayed a melting temperature (T_m) indicating thermoplastic behaviour.

Received 2nd March 2026,
Accepted 1st May 2026

DOI: 10.1039/d6py00213g

rsc.li/polymers

Introduction

The combination of depleting fossil fuel resources and increasing atmospheric carbon dioxide (CO_2) concentration has intensified the call for sustainability in all aspects of materials production. Transforming processes to use abundant renewable resources and afford a reduced carbon footprint is of great importance.[1–3] By replacing petrochemically-derived polymers with bio-derived alternatives, opportunity arises to build a 'circular plastics economy' where waste production is minimized.[2,4,5] Interest in renewable monomers from biomass feedstocks is rapidly growing, with studies on sources such as vegetable oils,[6] cellulose,[7] lignin,[8] and starch.[9] Additionally, a relatively new area of research has shown how terpenes, which are mainly derived from plants, can be modified to provide various monomers for the formation of polyurethanes, polyesters (PEs), polycarbonates (PCs), and more.[10–12] By reacting terpene-derived cyclic anhydrides with CO_2 and/or epoxides, new aliphatic PCs and/or PEs are formed that can contribute to a more sustainable plastics economy while also providing a method of indirect carbon storage within the polymer architecture.

Typically, commercial plastics contain a rigid/aromatic polymer backbone due to established syntheses and better chemical and physical properties compared to aliphatic polyesters and polycarbonates.[13–16] Therefore, to be commercially feasible, sustainable aliphatic polymers must be optimized to compete with existing methods. One way of achieving this is to create aliphatic polymers that can have their properties 'tuned' to a desired application. Ring-opening copolymerization (ROCOP) of epoxides and cyclic anhydrides and/or CO_2, is one example of how these polymers, such as polyesters and poly-

Department of Chemistry, Memorial University, St. John's, NL, Canada A1C 5S7. E-mail: fkerton@mun.ca

carbonates, can be formed.[17,18] Unfortunately, for polycarbonates, which typically exhibit high molecular weights and rigidities, this method has proved insufficient to replicate the physical properties of existing polymers.[19] However, when aliphatic polyesters and polycarbonates are combined to form a copolymer, either alternating, block, or random, there is the possibility of controlling the design of the polymer and, thereby, its chemical and physical properties. Properties such as glass transition temperature, crystallinity, and water solubility can be altered.[20–24]

A range of metal complexes have been studied for these types of polymerizations, particularly aluminum and zinc-based catalytic systems.[3,25–34] Specifically, Van Zee and Coates and coworkers presented metal salen (M = Cr, Co, and Al) catalysts for the copolymerization of PO and terpene-derived cyclic anhydrides. These systems yielded alternating polyester units with T_g values up to 109 °C, high molecular weights, and narrow dispersities.[18] In contrast, metal-free systems (*e.g.*, small organic molecules) for polymerization reactions are relatively underdeveloped yet exhibit certain advantages such as commercial availability, simplicity, and better selectivity and tunability.[35–38] Of particular interest to this work are organoboron catalysts, such as triethylborane, which has been shown to efficiently polymerize CO_2 and epoxides to produce polycarbonates and cyclic carbonates.[36,39–45] Similarly, Andrea *et al.* demonstrated tunable arylborane catalysis for the ROCOP of epoxides and CO_2, and also renewable anhydrides and epoxides, where the copolymerizations of vinylcyclohexene oxide (VCHO) and limonene oxide (LO) with phthalic anhydride (PAH) and *cis*-4-cyclohexene-1,2-dicarboxylic anhydride (CDA) were investigated.[46–48] In the original ROCOP work, vinylcyclohexene residues in the resulting polycarbonate were modified using Ru-catalysed olefin metathesis.[45] Herein, building on work from Andrea *et al.*, this work presents the sequential copolymerizations of various bio-derived cyclic anhydrides, epoxides, and CO_2 using catalytic triphenylborane (BPh_3) to produce tunable polyester-*block*-polycarbonates, and post-polymerization modification (PPM) of residual olefinic groups *via* photoinitiated thiol–ene 'click' chemistry.[49–52] Pre-functionalization, molecular weights up to 20.6 kDa were achieved with narrow dispersities and T_g values up to 101 °C. After functionalization, the polymers in this work exhibited changes in molecular weights, thermal properties, and hydrophilicity, demonstrating the ability for tailoring polymer properties.

Ultimately, it is critical during the design and optimization phases of the study to consider the sustainability of the process and product. For example, in this work, starting materials can be renewably sourced, alternative 'greener' solvents can be used for polymer synthesis and purification, microwave conditions were employed for process intensification, and the resulting polymer has potential chemical recyclability. In addition, the ability to modify polymer properties *via* photoinitiated functionalization provides an energy-efficient strategy to access a broader range of materials without the need for repeated polymer syntheses, supporting more resource-efficient and sustainable materials design.

Experimental section

Details on reagents used, instrumentation, methods and synthesis procedures are given in the SI.

Results and discussion

Monomer synthesis

Cyclic anhydrides were prepared *via* Diels Alder reactions between maleic anhydride and various terpenes based on the research of Van Zee and Coates,[18] but modified to employ microwave-assisted synthesis.[53] Monomers **M1**, **M2**, **M3**, and **M4** (Scheme 1) were produced from α-terpinene, isoprene, α-phellandrene, and myrcene, respectively, in excellent yields (see SI). **M1–M4** were characterized by ^{1}H NMR spectroscopy and revealed exclusively *endo*-selectivity (Fig. S1–S4).[18,54] Little to no purification was required of the monomers compared to literature methods using conventional heating,[18] and no by-products or impurities could be seen in their ^{1}H NMR spectra. This microwave-assisted approach means reaction times could be reduced from 16–36 h to 10 min, allowing for rapid, and more efficient, production of a suite of monomers. Additionally, the modified synthesis replaces diethyl ether with toluene as the reaction solvent, which has been deemed an overall 'greener' solvent.[55,56] To our knowledge, this is the first report of cyclic anhydride formation *via* microwave-assisted Diels Alder reactions from bio-derived terpenes.

Copolymerization reactions

The copolymerization of **M1–M4** was investigated using neat *cis*-cyclohexene oxide (CHO) and neat racemic propylene oxide (PO) in the presence of the Lewis acidic catalyst triphenylborane (BPh_3) and a co-catalyst bis(triphenylphosphine)iminium chloride (PPNCl) (Scheme 2). BPh_3 has previously been reported to be an efficient non-metal catalyst in the ROCOP of

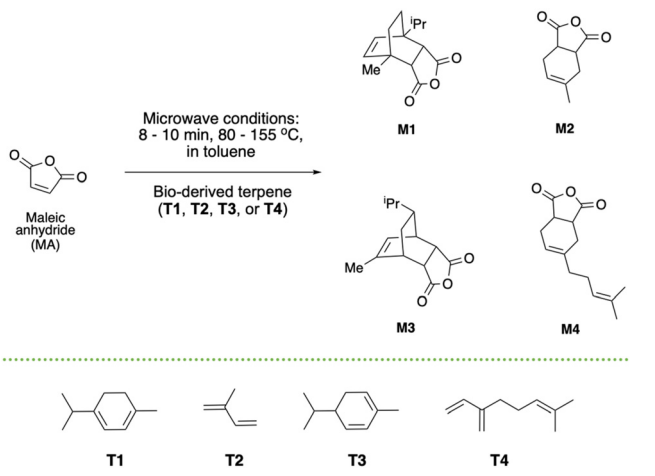

Scheme 1 Microwave-assisted synthesis of terpene-derived cyclic anhydrides. (**T1** = α-terpinene, **T2** = isoprene, **T3** = α-phellandrene, **T4** = myrcene).

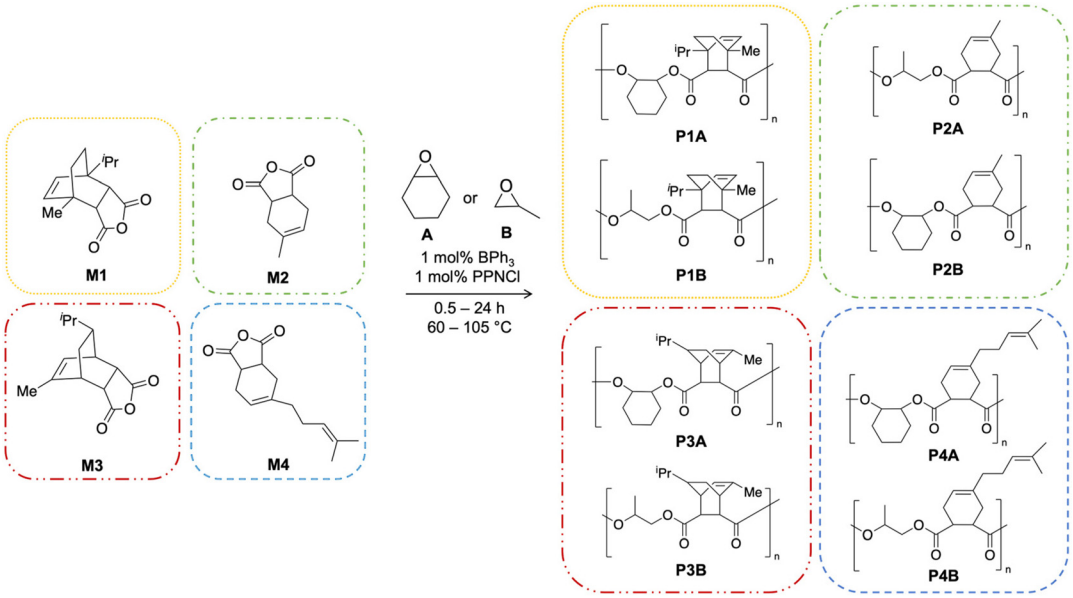

Scheme 2 Polymerizations of bio-derived cyclic anhydrides **M1–M4** with epoxides (CHO or PO) to form polyesters **P1A/B–P4A/B**. Reactions performed under N_2 atmosphere.

epoxides with CO_2 to form polycarbonates, and more recently with cyclic anhydrides to form polyesters.[46,48] In the current work, ROCOP was performed at various temperatures, monomer ratios, and times to optimize bio-derived cyclic anhydride conversion, molecular weight (M_n), and dispersity ($Đ$) with CHO and PO. These results are summarized in Table 1.

Degrees of polymerization reach up to 70 in terms of resulting ester groups, showing polymer formation in preference to oligomer formation. Polymers were characterized by gel per-

Table 1 Data obtained for polyesters produced by ring opening copolymerization (ROCOP) of epoxides and cyclic anhydrides **M1–M4**[a]

Entry	Cyclic anhydride	T (°C)	t (h)	% anhydride conversion[b]	M_n (kDa) ($Đ$)[c]	Theoretical M_n [d] (kDa)
Epoxide: CHO						
1	**M1**	105	24	>99	8.3 (1.72)	33.2
2	**M1**	80	24	58	6.9 (1.09)	19.2
3[e]	**M2**	80	24	>99	5.4 (1.10)	26.4
4	**M2**	80	4	>99	3.9 (1.12)	26.4
5[f]	**M3**	80	24	>99	6.2 (1.29)	33.2
6	**M3**	80	4	69	2.2 (1.27)	22.9
7[g]	**M4**	80	24	90	4.3 (1.36)	29.9
8	**M4**	60	24	88	3.7 (1.17)	29.3
Epoxide: PO						
9	**M1**	80	24	>99	9.4 (1.59)	29.0
10	**M1**	80	4	44	4.7 (1.13)	12.9
11	**M2**	80	24	>99	8.3 (1.66)	22.4
12	**M2**	80	4	<1	n.d.	n.d.
13	**M3**	105	24	97	13.4 (1.14)	25.7
14	**M3**	105	4	>99	12.1 (1.13)	29.2
15	**M3**	105	1.5	14	6.3 (1.42)	4.1
16	**M3**	80	24	>99	11.1 (1.75)	29.2
17	**M4**	105	1	97	2.6 (1.10)	29.2
18	**M4**	105	0.5	93	3.6 (1.05)	27.2
19	**M4**	80	24	97	5.0 (1.40)	28.4
20	**M4**	60	24	98	2.9 (1.14)	28.7

[a] All reactions were performed at a ratio of 1 : 1 : 100 : 500 [BPh_3]/[PPNCl]/[anhydride]/[epoxide] unless otherwise stated. [b] Determined *via* ^{1}H NMR spectroscopy. No ether linkages were observed unless otherwise indicated. [c] Determined by GPC in THF. M_n and $Đ$ were calculated using the Wyatt ASTRA software with dn/dc values acquired *via* off-line analysis ($Đ = M_w/M_n$). n.d. = not determined. [d] Theoretical M_n calculated by [(molecular weight of repeating unit) × (100 units of anhydride)] × % conversion by ^{1}H NMR spectroscopy. [e] Ester : ether linkage = 1 : 0.7, 59% ester selectivity, determined by ^{1}H NMR spectroscopy. [f] Ester : ether linkage = 1 : 0.2, 83% ester selectivity, determined by ^{1}H NMR spectroscopy. [g] Ester : ether linkage = 1 : 1, 50% ester selectivity, determined by ^{1}H NMR spectroscopy.

meation chromatography (GPC), matrix-assisted laser desorption ionization time-of-flight (MALDI-TOF) mass spectrometry, and $^{13}C\{^{1}H\}$, 1D and 2D ^{1}H NMR spectroscopy techniques.

Depending on the structure of the anhydride, high conversions could be achieved in <1 h with molecular weights up to 13.4 kDa and $Đ$ values of 1.05–1.75. The highest M_n was achieved with the α-phellandrene-derived monomer (**M3**) and PO (Table 1, entries 13–16) with 13.4 kDa. This increased M_n may be due to chain transfer after complete consumption of the anhydride, therefore, we performed reactions with shorter times to monitor M_n (Table 1, entries 14 and 15). After 1.5 h, the M_n was determined to be 6.3 kDa. Interestingly, the GPC traces for polymer obtained after 4 h were bimodal, whereas the polymer obtained initially (at t = 1.5 h) was monomodal (see Fig. S14).

MALDI-TOF mass spectra of the polyesters showed series corresponding to repeating units of combined cyclic anhydride and epoxide. A representative spectrum can be seen in Fig. 1 for the polyester (**P2A**) formed from CHO and **M2** (Table 1, entry 4). A repeating unit of cyclohexene oxide + cyclic anhydride ($C_6H_{10}O$ + $C_9H_{10}O_3$, 262.13 m/z) is observed corresponding to the expected polyester. End group analysis confirms the presence of –Cl, –OH, and –OCH_3 end groups.

The alpha methine region of the $^{13}C\{^{1}H\}$ NMR spectra was analyzed to confirm the relative stereochemistry of diester units. In this suite of reactions, two diagnostic resonances were observed between 40–55 ppm (polymer dependent), corresponding to literature values for *cis*-diester units (see Fig. S15).[18] For polyesters formed with racemic PO, the $^{13}C\{^{1}H\}$ NMR spectra revealed a sharp peak in the methine region (~68 ppm) indicating isotactic stereochemistry of the PO methyl groups (Fig. 2).[57,58]

Optical rotation analysis of unreacted PO post-polymerization suggests stereocenter inversion as the residual PO was not enantiomerically-enriched. For reactions with enantiomerically pure PO, full conversions and isotactic stereochemistry were observed for both *R* and *S* enantiomers, indicating no enantiomeric preference.

Typically, PO homo- and co-polymerizations achieve high stereocontrol by using bulky metal-based catalysts containing chiral sites, as seen by Coates and coworkers.[17,18,58,59] While Van Zee and Coates did not explicitly discuss this stereochemistry, the ^{13}C NMR spectra presented in their work shows multiple stereochemistries present.[18] Non-metal catalysts, specifically organoboron catalysts, have been seen to provide

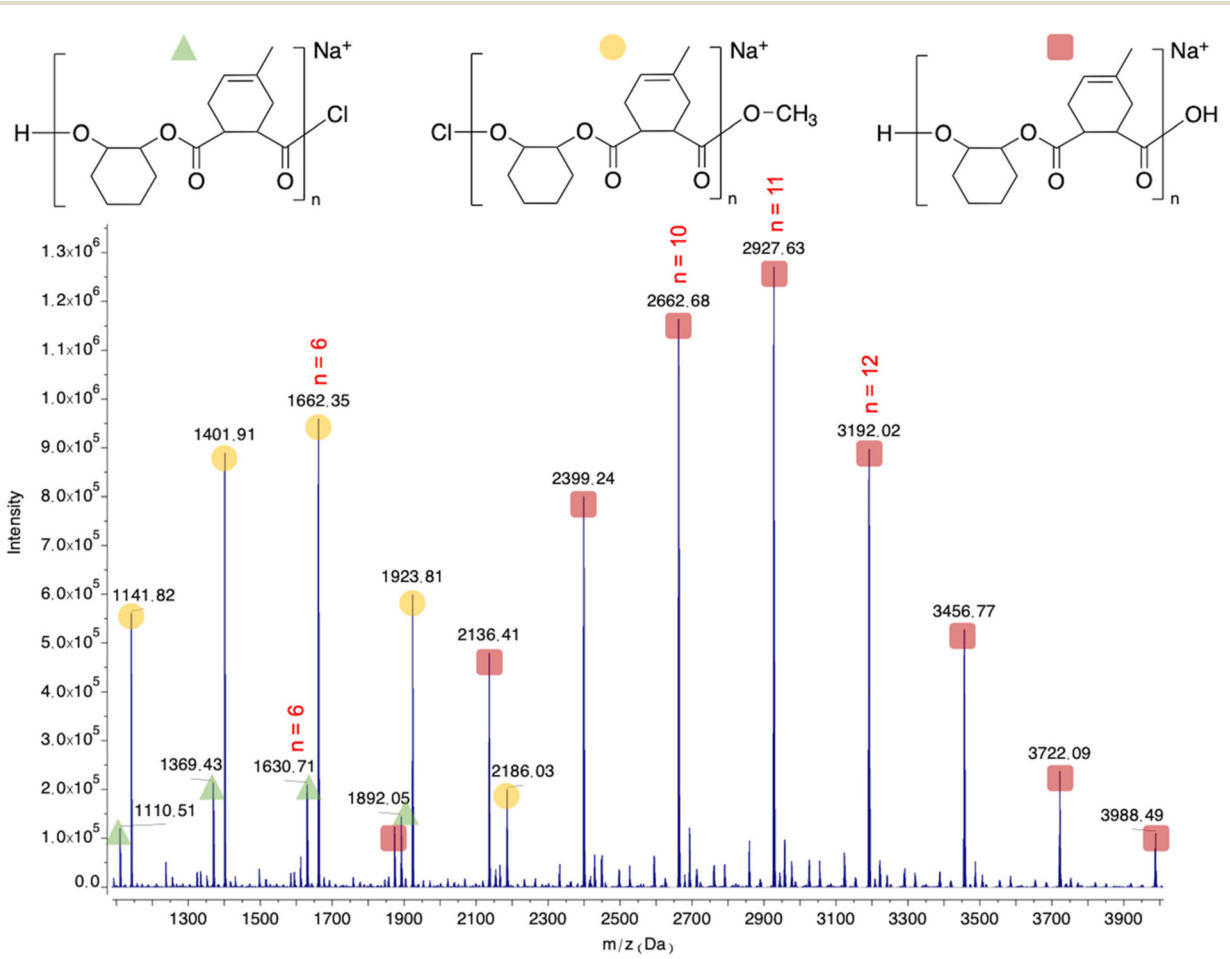

Fig. 1 Expanded region of MALDI-TOF spectrum for polyester formed from monomers CHO and **M2** (Table 1, entry 4). The spectrum shows a main series corresponding to the expected polyester with –OH, –Cl, and –OCH_3 end groups (red/square, illustrated).

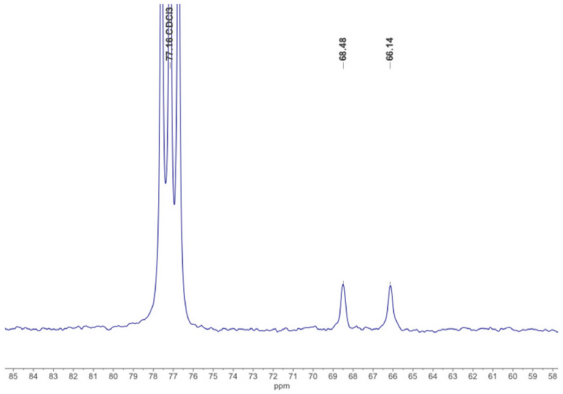

Fig. 2 Expanded methine region of $^{13}C\{^1H\}$ NMR spectrum of polyester formed from **M2** and PO (**P2B**; Table 1, entry 11). A single sharp peak at 68.48 ppm demonstrates isotacticity.

regio- and stereoselectivity for the homopolymerization of PO through the use of chiral sites.[60–62] In contrast, several non-chiral borane systems (*e.g.*, alkylboranes or arylboranes) have demonstrated high copolymerization ability of epoxides and CO_2 but do not present ^{13}C NMR spectra or stereoselectivity analyses of PO methyl groups.[36,43,44,48] Studies on the ROCOP of PO and maleic anhydride using BPh_3/PPNCl show the presence of two additional methine peaks (Fig. S16) indicative of multiple different regio- or stereochemistries. This suggests less stereocontrol when using a smaller, less sterically-demanding anhydride. Polymerizations of **M2** and PO performed at high (150 °C) and low (50 °C) temperatures also exhibit this stereocontrol *via* $^{13}C\{^1H\}$ NMR spectroscopy (Fig. S17 and S18). Therefore, we propose a 'monomer-controlled' mechanism as the source of stereoselectivity, where the stereochemistry of the previous anhydride monomer inserted influences the stereochemistry of the incoming monomer.

To understand the polymeric growth of the polyesters, a molecular weight growth study was performed (Fig. 3) using the optimized conditions from Table 1, entry 4 (**M2** and CHO) chosen due to its shorter reaction time. Aliquots were taken at regular time intervals and analyzed by GPC.

The analyses showed an induction period during the first 30 min of polymerization, most likely due to activation of the catalyst system. After the induction period, a linear growth trend is observed in molecular weight. Mass transfer effects due to increased viscosity towards the end of polymerizations likely led to lower than expected observed molecular weights after 175 min.

Sequential copolymerization reactions

Once experimental parameters for epoxide-anhydride ROCOP were optimized, sequential copolymerization reactions were attempted to form polyester-*block*-polycarbonate products (Scheme 3).

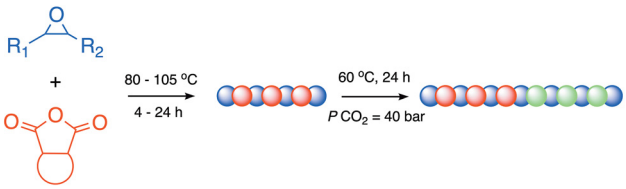

Scheme 3 General reaction scheme for BPh_3/PPNCl catalysed sequential Ring Opening Copolymerization (ROCOP) of epoxides, terpene-derived anhydrides, and CO_2 described in this work.

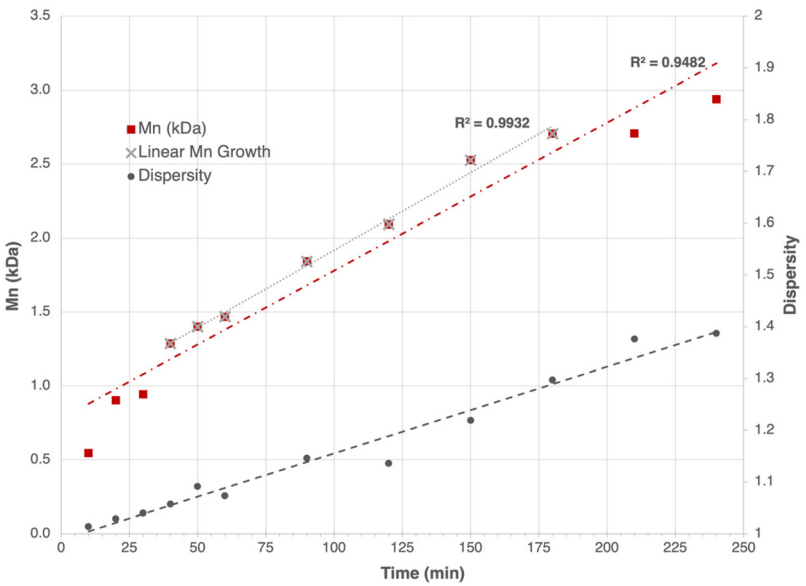

Fig. 3 Molecular weight and dispersity trends for polymerization of **M2** and CHO at 80 °C for 4 h. Results show a polymerization induction period, followed by linear M_n growth.

In our previous communication, only LO or VCHO with PAH and/or CDA were investigated using our catalyst system.[46] In a typical reaction, the epoxide and the anhydride were left to react under the optimized conditions for polyester formation described above. After that time, it was assumed that >99% anhydride monomer had been consumed and CO_2 was added to begin forming the polycarbonate block. The results of sequential block copolymerizations using anhydrides **M1**–**M4** with either CHO or PO to yield polyester-*block*-polycarbonates are presented in Table 2.

Characterization of the resulting copolymers was initially performed using ^{1}H NMR spectroscopy but proved insufficient to confirm the presence of polycarbonate linkages as the chemical shifts for the polyester peaks overlap with the expected methine peak from 4.5–5.0 ppm (Fig. S19).[39,63] However, ^{1}H NMR spectroscopy does show good selectivity for polymer formation as no evidence was seen for the cyclic carbonate product and minimal ether linkages. Further analyses *via* HSQC spectroscopy (Fig. 4) and MALDI-TOF MS (Fig. 5) were able to confirm the presence of carbonate linkages.

Comparing the HSQC spectrum to that of the corresponding polyester (Fig. S20) revealed a new correlation peak in the expected polycarbonate region that was assigned to the newly formed polycarbonate methine proton (4.39 ppm, peak in yellow square, Fig. 4).

The MALDI-TOF MS spectra for block copolymers were complex, but revealed several overlapping series with a repeating unit of 142 Da corresponding to a polycarbonate unit (Fig. 5). A one-pot experiment (Table 2, entry 4) was performed to determine whether block structure would still be obtained if all monomers were introduced at the same time. This method still led to >99% anhydride conversion by ^{1}H NMR spectroscopy, but revealed lower M_n polymer formation by GPC. Analysis of the MALDI-TOF mass spectrum revealed a less controlled polymerization ultimately leading to a random copolymer with two main distributions (see Fig. S21) in contrast to a single Gaussian distribution of peaks observed for the block copolymer (Fig. 5).

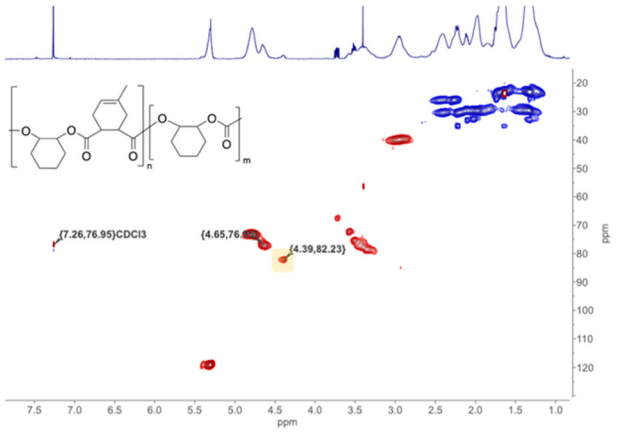

Fig. 4 HSQC spectrum (500 MHz, $CDCl_3$) of polyester-*block*-polycarbonate formed from anhydride **M2**, CHO, and CO_2 (Table 2, entry 3). New correlation peak highlighted in yellow square (4.39 ppm, 82.23 ppm).

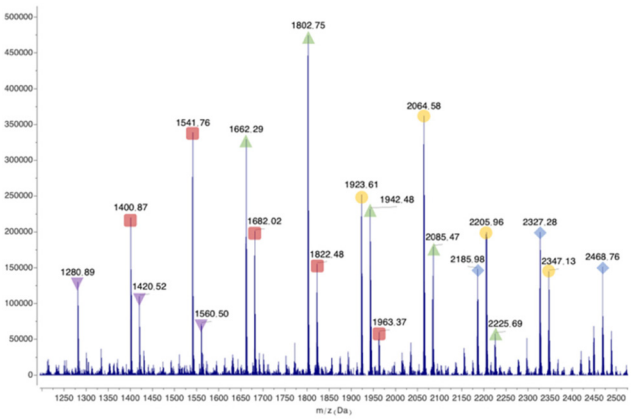

Fig. 5 Expanded region of MALDI-TOF mass spectrum of polyester-*block*-polycarbonate polyester formed from anhydride **M2**, CHO, and CO_2 (Table 2, entry 3). Each labelled series corresponds to polycarbonate units of 142 *m*/*z* (illustrated).

Table 2 Data obtained for ROCOP of cyclic anhydride, epoxide, and CO_2 [a]

Entry	Polymer	Cyclic anhydride	Epoxide	*T* (°C)	*t* (h)	M_n (kDa) PE[b]	M_n (kDa) PC[b]	$Đ$[b]	% PE[b] (avg)	Diffusion Coeff. ($\times10^{-10}$, m^2 s^{-1}, D)[c]
1	**P1A**	**M1**	CHO	105	24	<1	7.35	1.16	<5	2.09
2[d]	**P1B**	**M1**	PO	80	24	9.2	n.d.	1.11	>99	1.61
3	**P2A**	**M2**	CHO	80	2	4.05	2.37	1.09	63	2.67
4[e]	**P2A**	**M2**	CHO	80	24	2.39	1.80	1.09	57	n.d.
5[d]	**P2B**	**M2**	PO	80	24	7.28	1.21	1.40	86	2.35
6[f]	**P3A**	**M3**	CHO	80	24	n.d.				2.48
7[d]	**P3B**	**M3**	PO	80	24	5.72	15.9	1.03	26	1.97
8	**P4A**	**M4**	CHO	80	24	1.48	3.69	1.53	32	2.21
9[d,f]	**P4B**	**M4**	PO	105	1	n.d.	1.97			

[a] All reactions were performed at a ratio of 1 : 1 : 100 : 500 [BPh_3]/[PPNCl]/[anhydride]/[epoxide] ratio. All polycarbonate reactions were conducted at 60 °C, under 40 bar of CO_2 for 24 h, unless otherwise stated. [b] Determined by GPC in THF. M_n and $Đ$ were calculated using the Wyatt ASTRA software with d*n*/d*c* values acquired *via* off-line analysis ($Đ = M_w/M_n$). Polyester (PE) and polycarbonate (PC) fractions were determined *via* ASTRA 8 software conjugate analysis methods. [c] Performed in $CDCl_3$ at 298 K. [d] Initiated with 5 molar equivalents of CHO. [e] Performed as a one pot polymerization where all monomers were added at the same time. [f] GPC conjugate analyses were unsuccessful for these samples, not determined (n.d.).

Additionally, analysis of each block copolymer *via* diffusion-ordered NMR spectroscopy (DOSY) showed that all signals within a spectrum had the same diffusion coefficient, giving confidence that a single chain polymer product was formed (Fig. 6).

Supplementary analyses *via* FT-IR spectroscopy was performed to compare the carbonyl stretch (~1730 cm^{-1}) of polyesters and block copolymers. Ideally, a second carbonyl stretch will be observed for the block copolymers due to the newly added carbonate group. In Fig. 7, the carbonyl peaks are presented for isolated products anhydride **M2**, polyester **P2A**, and its corresponding polyester-*block*-polycarbonate. Initial observations show a shift in wavenumber of the carbonyl stretch of all three species, as well as an increase in the full width at half maximum in the block copolymer (green). This increase, along with the deconvolution of the peak (see Fig. S32), gives confidence for the incorporation of a carbonyl stretch in a new environment.

GPC analysis was used to characterize the polyesters formed, as mentioned previously.

For the corresponding block copolymers, GPC analysis was initially performed using the refractive index increment value (d*n*/d*c*) of the corresponding polyester to compare molecular weights. However, due to the expected distinct segments in the polymers, using such d*n*/d*c* values technique would likely lead to inaccuracies in molecular weight determination. Therefore, polymer conjugate analysis was performed on the block copolymers formed in this work (Fig. 8).[64,65] Molecular weights (M_n) of polyester and polycarbonate segments were obtained and are presented in Table 2. To compare, M_n values of block copolymers were also calculated using the corresponding polyester d*n*/d*c* value and are presented in Table S1.

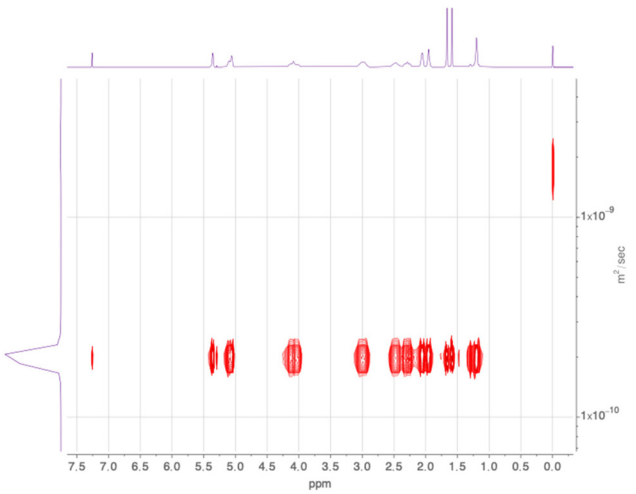

Fig. 6 DOSY NMR spectrum of polyester-*block*-polycarbonate formed from anhydride **M4**, PO, and CO_2 (Table 2, entry 9) in $CDCl_3$ at 298 K. Data obtained from analysis of DOSY NMR spectrum: D = 1.97 × 10^{-10} m^2 s^{-1}.

Thermal analyses

Characterization by DSC was performed on polyesters and block copolymers of comparable molecular weight to determine thermal properties, such as glass transition temperatures (T_g) (Table 3). For both polyesters and block copolymers, no melting or crystallisation curves were observed before reaching decomposition temperatures, indicating fully amorphous materials.[66,67] Due to the structural similarity of monomers, the polyester and polycarbonate blocks are sufficiently miscible, resulting in one observed T_g for the block copolymers (Fig. 9).[68] The T_g of the polyesters range from 1.5 °C (Table 3, entry 8) to 101 °C (Table 3, entry 1). The wide range can be partially explained by the interactions between different polymer chains. In the case of anhydride **M3**, the PO-based polyester exhibited a higher T_g than the CHO-based polyester, which was unexpected (Table 3, entry 6). This result is most likely due to the much higher molecular weight of the PO-based polymer.

Another unexpected observation was the relatively low T_g of the myrcene-based polyesters with PO compared to the polyesters incorporating other terpenes. This result is most likely

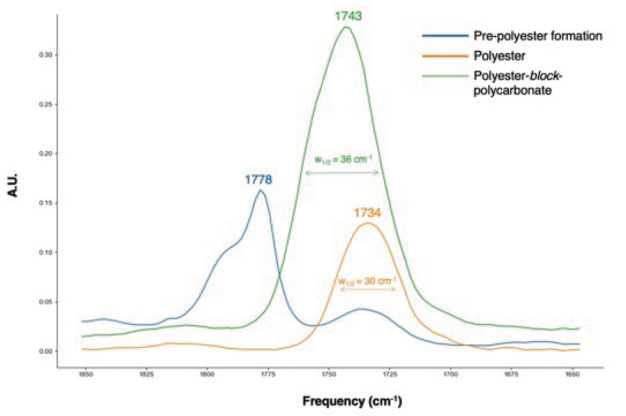

Fig. 7 FT-IR spectra of carbonyl stretching frequencies for anhydride **M2** (blue), polyester **P2A** (orange), and its corresponding polyester-*block*-polycarbonate (green).

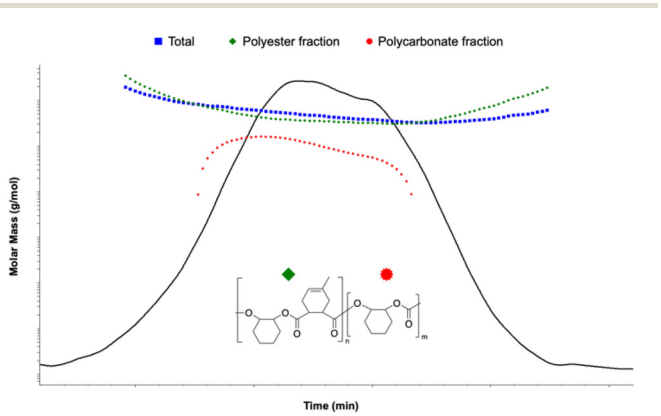

Fig. 8 GPC light scattering trace demonstrating molecular weight fractions of polyester-*block*-polycarbonate (Table 2, entry 3). Fractions determined *via* ASTRA software (Wyatt) GPC conjugate analysis method.

Table 3 Glass transition temperature comparisons between polyesters and polyester-*block*-polycarbonates[a]

Entry	Cyclic anhydride	Epoxide	T (°C)	t (h)	Polyester T_g (°C)	Polyester-*block*-polycarbonate T_g (°C)	ΔT_g (°C)	Possible explanation
1	**M1**	CHO	105	24	79.6	59.5	−20.1	↓packing ability = ↓T_g
2	**M1**	PO	80	24	76.8	75.9	−0.9	Addition of small PO comonomer ↑flexibility = ↓T_g
3	**M2**	CHO	80	2	69.6	82.6	+13.0	Addition of harder PCHC block ↑packing/rigidity = ↑T_g
4	**M2**	PO	80	24	32.4	30.0	−2.4	Addition of small PO comonomer ↑flexibility = ↓T_g
5	**M3**	CHO	80	24	78.1	96.6	+18.5	Addition of harder PCHC block ↑rigidity = ↑T_g
6	**M3**	PO	80	24	78.5	76.3	−2.2	Addition of small PO comonomer ↑flexibility = ↓T_g
7	**M4**	CHO	80	24	101	72.9	−28.1	↓packing ability ↑flexibility = ↓T_g
8	**M4**	PO	105	1	1.5	4.1	+2.6	May experience chain entanglement ↑rigidity = ↑T_g

[a] All DSC analyses were performed using the same method of −80 °C–300 °C at a ramp rate of 10 °C min^{-1}, cycled 3 times. T_g was taken from the second cycle using inflection midpoints.

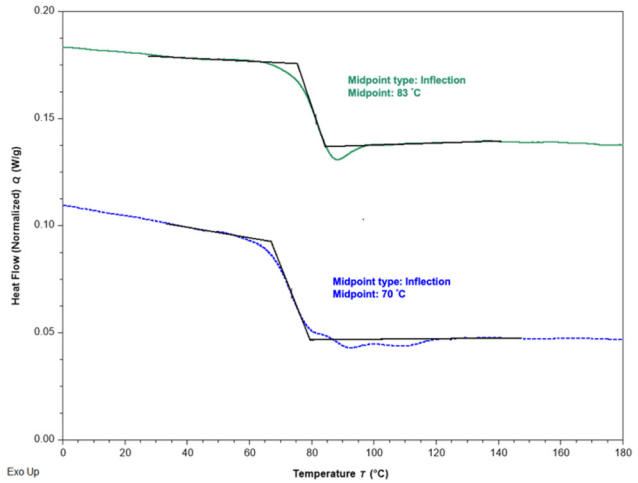

Fig. 9 Glass transition temperature analyses of polyester (blue, bottom) and polyester-*block*-polycarbonate (green, top) made with **M2** and CHO (Table 3, entry 3).

due to the poor packing ability (due to side chains) and relatively high flexibility of the polymer backbone.

In comparison, Kleij and coworkers observed T_g values ranging from 53–165 °C for the ROCOP of terpene oxides and a more rigid cyclic anhydride, PAH, using a monometallic Fe-based catalyst.[13,31] A more relevant comparison can be made with the work of Sanford *et al.* where high T_g values (up to 184 °C) for aliphatic polyesters with monomers **M1** or **M3** and CHO or PO were reported.[54] They saw that polyesters formed with bulkier anhydrides resulted in higher T_g values, as expected, which is also seen in this work. The differences observed in T_g values between their polymers and those reported herein may result from the lower molecular weights obtained in the current study.[54]

When using CHO as a monomer, some copolymers exhibited a decrease in T_g when the polycarbonate block was added (Table 3, entries 1 and 7). This was a surprising result as it has been reported that the polycarbonate derived from CO_2 and CHO (PCHC) can have T_g values up to 116 °C.[69] A possible explanation for this decrease is that the addition of the PCHC block creates large gaps in the polymer matrix, decreasing the packing ability of the polymer chains. Interestingly, an increase in T_g (+18.5 °C) was observed when the PCHC block was added to the α-phellandrene/CHO – based polyester (Table 3, entry 5). This increase could be attributed to entanglement between chains caused by the side chains on the α-phellandrene – derived monomer. However, modelling studies would need to be performed in order to fully understand the increases and decreases in T_g for the block copolymers described here.

When PO is used, all copolymers analyzed resulted in a T_g close to that of PPC (measured to be 24 °C). It's probable that the addition of PPC units likely increases flexibility of the polymer (Table 3, entries 2, 4, and 6) and causes a lower T_g value, or the addition of the PPC block to polyesters with long side chains increases the amount of polymer chain entanglement and, therefore, increases the T_g (Table 3, entry 8).

Functionalization of polymers by thiol–ene chemistry

Post-polymerization modification (PPM) *via* thiol–ene click chemistry provides an efficient route to tailor polymer properties and target specific applications. These modifications proceed *via* a radical mechanism that can be thermally or photochemically induced.[70] Recently, Darensbourg and coworkers demonstrated a one-pot double thermal PPM of their biobased polyesters with amine and thiol groups.[71] More similar to this work, Kleij and coworkers have demonstrated thermally initiated PPM of terpene-derived polymers with >95% degree of functionalization.[3] Alternatively, Haddleton and coworkers showed a photochemical PPM of poly(geranyl acrylate) with thiols that yielded higher molecular weight polymers with differing thermal properties.[51]

In this work, 3-mercaptopropionic acid (3MPA) and butyl 3-mercaptopropionate (B3MP) were chosen as the PPM thiols and 2,2-dimethoxy-2-phenylacetophenone (DMPA) as the photoinitiator (Scheme 4). The resulting functionalized polyesters were characterized by ^{1}H NMR spectroscopy, DSC, TGA, elemental analysis, and GPC. These results are summarized in Table 4. Initial observations saw that polymers functionalized with 3MPA exhibited differing solubilities compared with the original polyesters, which is not surprising given the addition of the hydrogen-bond donating functional group (–COOH).

The degree of functionalization (DF, %) was determined by relative integrations of the olefinic peak (between 5.4–6.0 ppm) in the polyester compared to the methine protons (between 5.0–5.4 ppm) in the ^{1}H NMR spectra (Fig. S33–42). DF was found to be especially high for isoprene- and myrcene-derived polymers regardless of the thiol used. For terpinene-derived polyesters, high DF was seen when using 3MPA (Table 4, entries 1 and 3), whereas the larger thiol B3MP yielded a DF <65%. Interestingly, functionalization attempts with the phellandrene-derived polyesters were relatively unsuccessful, yielding limited PPM (1–20% DF, see Table S2) Related work by Coates and coworkers observed that both terpinene- and phellandrene-derived polyesters were unreactive towards AIBN/heat catalyzed orthogonal thiol–ene functionalization.[72] Therefore, it is interesting to see that photoionization seems to be key in functionalizing terpinene-derived polyesters, but is still not sufficient for the more hindered olefin sites of the phellandrene-derived polyesters.

In addition, elemental analysis of the newly formed polymers was performed to confirm the presence of the sulfur functional group. Results matched closely with the expected sulfur composition (see Table S3), with the exceptions of Table 4, entry 5, which has a much higher %*S* than expected, and entry 14, which has a lower than expected %*S* based on calculations.[73] It is possible that these values are due to random error, as noted in the study by Kuveke *et al.*[74]

Depending on the DF and the chosen thiol, we predict that the wettability of the surface will change accordingly. When functionalized with 3MPA, which contains a –COOH functional group, it is expected that the resulting surface will be more hydrophilic. Similarly, when B3MP, which includes a long chain alkyl group, the surface should increase in hydrophobicity.[75] Exemplar surface contact angle measurements were taken of polyester **P2A** (due to >99% DF) and its functionalized analogues to observe any changes in hydrophilic character (Fig. 10). The non-functionalized precursor, **P2A**, exhibited a surface contact angle with water of 71°, indicating a relatively hydrophobic surface. When functionalized with 3MPA, the surface contact angle decreases to 59°, signifying a more hydrophilic surface due to the water droplet spreading further along the surface.[75] Likewise, when B3MP is used, the contact angle increases to 103°, suggesting a more hydrophobic surface than its precursor.

As expected, the molecular weight of the functionalized polymers increased along with a slight increase in dispersity and aligns well with the predicted M_n values of PPM functionalized based on the degree of substitution and the molar mass of the thiol. The exception is when **P4A** is functionalized with either thiol (Table 4, entries 9 and 10), where the measured M_n is much greater than expected. Agglomeration in solution is a possibility, but further investigation for these higher than expected M_n values is required.

Thermal analyses *via* TGA and DSC of the newly formed functional polymers yielded interesting results. High decomposition temperatures ($T_{d,onset}$) near 300 °C were observed, close to the decomposition of PCHC, allowing for high temperature applications.[76] However, when **P2B** was functionalized with B3MP (Table 4, entry 8), the $T_{d,onset}$ is much lower (119 °C) than others. A much lower T_g was also observed for this polymer (T_g = 5 °C), indicating a soft and more rubbery material. Contrarily, and relatively high T_g (T_g = 135 °C) is observed when **P1A** was functionalized with 3MPA (Table 4, entry 1) with higher thermal stability ($T_{d,onset}$ = 318 °C), demonstrating a more rigid material.

Intriguingly, when **P2A** is functionalized with 3MPA (Table 4, entry 5), no T_g was observed. Instead, a melting tran-

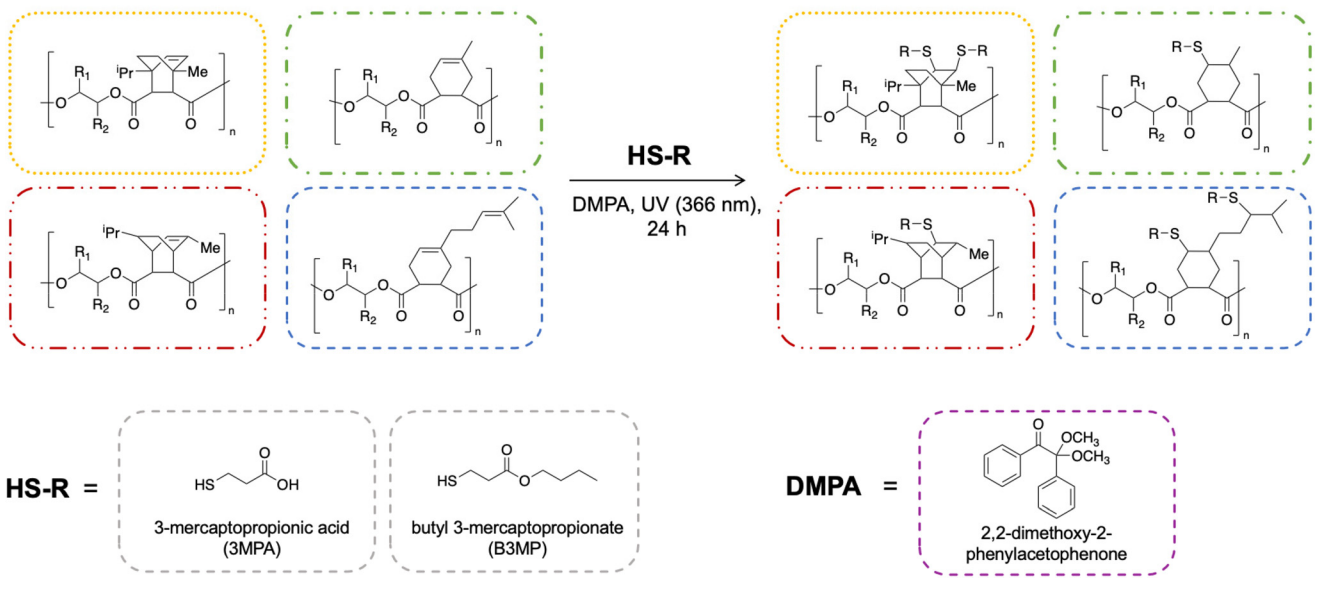

Scheme 4 General thiol–ene functionalization of polyesters from **M1–M4** using 2,2-dimethoxy-2-phenylacetophenone (DMPA) as the photoinitiator.

Table 4 Functionalization of polyesters in this work with photoinitiated thiol–ene click chemistry[a]

Entry	Polyester	Thiol	DF[b] (%)	Polyester T_g[c] (°C)	Functionalized T_g[c] (°C)	T_d[d] (°C)	GPC M_n [Theor. M_n][e] (kDa)	$Đ$[e]	%S[f]
1	**P1A**	3MPA	90	80	135	318	12.1 [13.1]	1.44	7.19
2		B3MP	65		63	313	10.5 [13.6]	1.38	5.48
3	**P1B**	3MPA	85	77	82	304	14.7 [15.1]	1.44	8.33
4		B3MP	60		27	296	10.7 [15.6]	1.46	5.76
5	**P2A**	3MPA	>99	70	N/A (T_m = 138)	207	14.3 [8.1]	1.13	19.15 [8.36]
6		B3MP	>99		52	316	8.9 [8.5]	1.25	7.12
7[g]	**P2B**	3MPA	80	32	23	318	—	—	8.39
8[g]		B3MP	>99		5	119	—	—	8.24
9	**P4A**	3MPA	>99/80	101	34	208	11.0 [7.3]	1.25	10.18
10		B3MP	>99/70		63	304	49.2 [6.3]	1.35	3.60

[a] All functionalization reactions were performed at 22 °C with DMPA as the photoinitiator in a 1 : 10 : 0.1 (polyester : thiol : DMPA) molar ratio for 24 h. n.d. = not determined. [b] Degree of functionalization (DF) (%) of pendant double bonds; obtained *via* ^{1}H NMR spectroscopy. [c] DSC analyses performed from −80 to 150 °C, cycled three times at 10 °C min^{-1}. T_g taken from second cycle using inflection midpoints. [d] TGA analyses performed from 25 °C–500 °C at 10 °C min^{-1}. Decomposition temperatures presented as the onset temperature. [e] Determined by GPC in THF. M_n and $Đ$ were calculated using the Wyatt ASTRA software with dn/dc values acquired *via* off-line analysis ($Đ = M_w/M_n$). Theoretical M_n calculated by [DF × [(DP of polyester) × (MW of functionalized repeating unit)] + [(100% − DF) × (MW of non-functionalized repeating unit)]]. [f] Determined *via* elemental analysis. Value in parentheses calculated from ^{1}H NMR spectroscopy using functional group protons compared to protons from polymer backbone. [g] GPC analyses were unsuccessful for these samples.

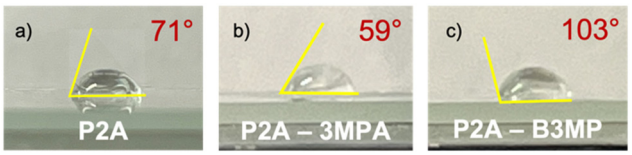

Fig. 10 Surface contact angle measurements of (a) isoprene/CHO derived polyester (**P2A**), (b) **P2A** functionalized with thiol 3MPA, and (c) **P2A** functionalized with thiol B3MP. Relative humidity = 54%.

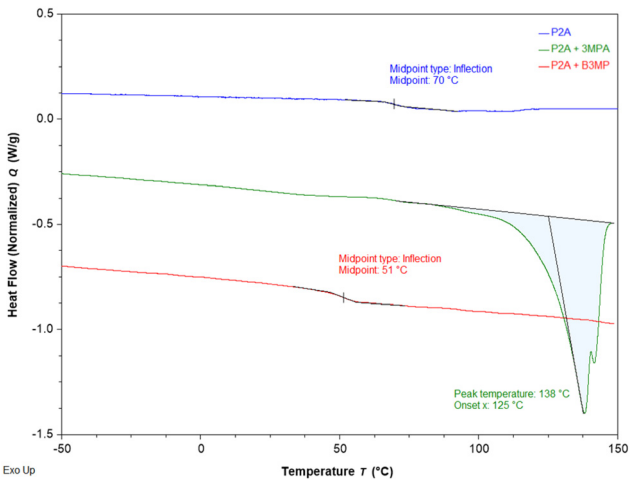

Fig. 11 DSC Overlay of **P2A** (top, blue), **P2A** functionalized with 3MPA (middle, green), and **P2A** functionalized with B3MP (bottom, red).

sition is seen at 138 °C (see Fig. 11), signifying a more ordered and crystalline polymer. For the polyester-*block*-polycarbonate materials that were formed previously, the polymer formed from the isoprene-derived anhydride and CHO was chosen as an exemplar block polymer due to its relatively equal composition of polyester and polycarbonate. To determine the stability of the functionalized block copolymer, DSC and TGA analyses were performed and are presented in Table 5. For both 3MPA and B3MP modification, a high T_d is seen with a decrease in T_g from the starting polyester (T_g = 59 °C (3MPA) and 44 °C (B3MP), precursor T_g = 83 °C). This indicates a thermally stable yet more disordered material has formed. Interestingly, when using 3MPA (Table 5, entry 1), the block copolymer did not yield a melting transition as the polyester had (Table 4, entry 5). Further analysis and investigation into the properties of the modified block copolymers is required and ongoing.

Table 5 Functionalization of polyester-*block*-polycarbonate from isoprene-derived anhydride, CHO and CO_2 with photoinitiated thiol–ene click chemistry[a]

Entry	Thiol	DF[b] (%)	Block copolymer T_g[c] (°C)	Func. T_g[c] (°C)	T_d[d] (°C)
1	3MPA	>99	83	59	307
2	B3MP	70		44	318

[a] All functionalization reactions were performed at 22 °C with DMPA as the photoinitiator in a 1 : 10 : 0.1 (polyester : thiol : DMPA) molar ratio for 24 h. [b] Degree of functionalization (DF, %) of pendant double bonds; obtained *via* ^{1}H NMR spectroscopy. [c] DSC analyses performed from −80 to 150 °C, cycled three times at 10 °C min^{-1}. T_g taken from second cycle using inflection midpoints. [d] TGA analyses performed from 25 °C–500 °C at 10 °C min^{-1}. Decomposition temperatures presented as the onset temperature.

Conclusions

A series of bio-derived stereoregular polyesters and polyester-*block*-polycarbonates were produced using terpene-derived cyclic anhydrides, epoxides, and CO_2 with a metal-free triphenylborane catalyst system. Conditions for polyester formation between cyclic anhydride and epoxides were first optimized to

achieve full anhydride conversions, molecular weights up to 13.4 kDa, and dispersities ranging from 1.05 to 1.72 by GPC. Once polyester formation conditions were optimized, sequential block copolymerizations were attempted by adding CO_2 to excess epoxide in a pressure vessel, P_{CO_2} = 40 bar. Polyester-*block*-polycarbonates were formed with molecular weights up to 20 kDa and dispersities ranging from 1.05 to 1.75 by GPC. Structure confirmation proved to be challenging by 1D NMR spectroscopy alone, but the combination of 1D and 2D NMR spectroscopy techniques and MALDI-TOF MS confirmed block copolymer structure.

Stereocontrol during polymerizations was observed resulting in isotactic polymers with *cis*-diester groups, as confirmed by $^{13}C\{^1H\}$ NMR spectroscopy, and is proposed to occur by chain-end control. Future studies will be performed to confirm the origin of stereoselectivity.

Furthermore, the polymers formed in this study were subjected to thiol–ene functionalization of the residual olefin (s). This yielded polymers with increased molecular weights and drastically different solubilities, surface contacts angles, and thermal properties compared with the original polymers.

Interestingly, it was seen that polyesters derived from α-terpinene were successful in their thiol–ene modifications *via* photoinitiation herein, unlike when thermal initiation has been employed.[72]

Additionally, an observed melting point for isoprene- and CHO-derived polyesters indicates the potential for melt processing, unlike any other polymers produced in this work.

Given the potential for this synthesis to be fully bio-derived, stereoselective, and afford polymers with good thermal stability, we will continue to focus on this research to determine potential polymer applications and improve process sustainability. More post-polymerization modification of the residual olefin groups will be investigated to further tune polymer properties.

Author contributions

F. M. K and M. D. S. W conceived the idea for project. M. D. S. W drafted the manuscript. M. D. S. W, A. M. C, A. P. K, and M. L. G performed experiments, characterization (NMR spectroscopy, FT-IR spectroscopy, GPC, MALDI-TOF MS, TGA, and DSC), and data analysis. All authors have given approval to the final version of the manuscript.

Conflicts of interest

The authors declare no competing financial interest.

Data availability

The data supporting this article have been included as part of the supplementary information (SI). Experimental details, NMR spectra, GPC traces, DSC and TGA thermograms and IR spectra are available. See DOI: https://doi.org/10.1039/d6py00213g.

Acknowledgements

F. M. K acknowledges financial support from Natural Sciences and Engineering Research Council of Canada (NSERC) for a Discovery and a CREATE Grant, Memorial University, the Canada Foundation for Innovation, and the Government of Newfoundland and Labrador. M. D. S. W thanks NSERC for a Canada Graduate Scholarship (Doctoral) and a Collaborative and Research Training Experience (CREATE) program (CIRCUIT), and Memorial University for Dr Liqin Chen Graduate Scholarships. A. M. C. thanks Mitacs for a Fulbright Canada-Mitacs Globalink Research Internship. We thank Memorial University's CREAIT Network for their support with this work.

References

1 A. Brandolese and A. W. Kleij, *Acc. Chem. Res.*, 2022, **55**, 1634–1645.
2 J.-G. Rosenboom, R. Langer and G. Traverso, *Nat. Rev. Mater.*, 2022, **7**, 117–137.
3 T. Senthamarai, E. Lanaro, J. Tinker, A. Buchard and A. W. Kleij, *Polym. Chem.*, 2025, **16**, 2784–2790.
4 T. Keijer, V. Bakker and J. C. Slootweg, *Nat. Chem.*, 2019, **11**, 190–195.
5 Y. Zhu, C. Romain and C. K. Williams, *Nature*, 2016, **540**, 354–362.
6 J. Thomas and R. Patil, *Ind. Eng. Chem. Res.*, 2023, **62**, 1725–1735.
7 A. A. B. Omran, A. A. B. A. Mohammed, S. M. Sapuan, R. A. Ilyas, M. R. M. Asyraf, S. S. Rahimian Koloor and M. Petrů, *Polymers*, 2021, **13**, 231.
8 A. Ghorai and H. Chung, *Adv. Funct. Mater.*, 2024, **34**, 2403035.
9 K. J. Falua, A. Pokharel, A. Babaei-Ghazvini, Y. Ai and B. Acharya, *Polymers*, 2022, **14**, 2215.
10 F. D. Monica and A. W. Kleij, *Polym. Chem.*, 2020, **11**, 5109–5127.
11 P. Holzmüller, C. Gardiner, J. Preis and H. Frey, *Macromolecules*, 2024, **57**, 5358–5367.
12 M. E. G. Mosquera, G. Jiménez, V. Tabernero, J. Vinueza-Vaca, C. García-Estrada, K. Kosalková, A. Sola-Landa, B. Monje, C. Acosta, R. Alonso and M. Á. Valera, *Sustainable Chem.*, 2021, **2**, 467.
13 L. Peña Carrodeguas, C. Martín and A. W. Kleij, *Macromolecules*, 2017, **50**, 5337–5345.
14 H. Li, H. Luo, J. Zhao and G. Zhang, *Macromolecules*, 2018, **51**, 2247–2257.
15 E. H. Nejad, A. Paoniasari, C. E. Koning and R. Duchateau, *Polym. Chem.*, 2012, **3**, 1308–1313.

16 S. Fujiki, K. Amaike, A. Yagi and K. Itami, *Nat. Commun.*, 2022, **13**, 5358.
17 J. M. Longo, M. J. Sanford and G. W. Coates, *Chem. Rev.*, 2016, **116**, 15167–15197.
18 N. J. Van Zee and G. W. Coates, *Angew. Chem., Int. Ed.*, 2015, **54**, 2665–2668.
19 S. Paul, Y. Zhu, C. Romain, R. Brooks, P. K. Saini and C. K. Williams, *Chem. Commun.*, 2015, **51**, 6459–6479.
20 E. Brulé, J. Guo, G. W. Coates and C. M. Thomas, *Macromol. Rapid Commun.*, 2011, **32**, 169–185.
21 H.-A. Klok and S. Lecommandoux, *Adv. Mater.*, 2001, **13**, 1217–1229.
22 S. Paul, C. Romain, J. Shaw and C. K. Williams, *Macromolecules*, 2015, **48**, 6047–6056.
23 T. Stosser and C. Williams, *Angew. Chem., Int. Ed.*, 2018, **57**, 6337–6341.
24 D. J. Darensbourg and F.-T. Tsai, *Macromolecules*, 2014, **47**, 3806–3813.
25 T. Chen, Y. Zhu and C. Williams, *Macromolecules*, 2018, **51**, 5346–5351.
26 W. T. Diment, W. Lindeboom, F. Fiorentini, A. C. Deacy and C. K. Williams, *Acc. Chem. Res.*, 2022, **55**, 1997–2010.
27 D. R. Moore, M. Cheng, E. B. Lobkovsky and G. W. Coates, *J. Am. Chem. Soc.*, 2003, **125**, 11911–11924.
28 Y. C. A. Sokolovicz, A. Buonerba, C. Capacchione, S. Dagorne and A. Grassi, *Catalysts*, 2022, **12**, 970.
29 F. Santulli, F. Tufano, M. Cozzolino, I. D'Auria, M. Strianese, M. Mazzeo and M. Lamberti, *Dalton Trans.*, 2023, **52**, 14400–14408.
30 W. Gruszka, L. C. Walker, M. P. Shaver and J. A. Garden, *Macromolecules*, 2020, **53**, 4294–4302.
31 F. D. Monica and A. W. Kleij, *ACS Sustainable Chem. Eng.*, 2021, **9**, 2619–2625.
32 H. Plommer, J. N. Murphy, L. N. Dawe and F. M. Kerton, *Inorg. Chem.*, 2019, **58**, 5253–5264.
33 E. D. Cross, G. K. Tennekone, A. Decken and M. P. Shaver, *Green Mater.*, 2013, **1**, 79–86.
34 A. C. Deacy, C. B. Durr and C. K. Williams, *Dalton Trans.*, 2019, **49**, 223–231.
35 D. Ryzhakov, G. Printz, B. Jacques, S. Messaoudi, F. Dumas, S. Dagorne and F. L. Bideau, *Polym. Chem.*, 2021, **12**, 2932–2946.
36 C. Zhang, X. Geng, X. Zhang, Y. Gnanou and X. Feng, *Prog. Polym. Sci.*, 2023, **136**, 101644.
37 M. J.-L. Tschan, R. M. Gauvin and C. M. Thomas, *Chem. Soc. Rev.*, 2021, **50**, 13587–13608.
38 G.-W. Yang, Y. Wang, H. Qi, Y.-Y. Zhang, X.-F. Zhu, C. Lu, L. Yang and G.-P. Wu, *Angew. Chem., Int. Ed.*, 2022, **61**, e202210243.
39 D. Zhang, S. Boopathi, N. Hadjichristidis, Y. Gnanou and X. Feng, *J. Am. Chem. Soc.*, 2016, **138**, 11117–11120.
40 L.-F. Hu, C.-J. Zhang, H.-L. Wu, J.-L. Yang, B. Liu, H.-Y. Duan and X.-H. Zhang, *Macromolecules*, 2018, **51**, 3126–3134.
41 S. Liu, T. Bai, K. Ni, Y. Chen, J. Zhao, J. Ling, X. Ye and G. Zhang, *Angew. Chem., Int. Ed.*, 2019, **58**, 15478–15487.
42 J.-L. Yang, H.-L. Wu, Y. Li, X.-H. Zhang and D. J. Darensbourg, *Angew. Chem., Int. Ed.*, 2017, **56**, 5774–5779.
43 V. K. Chidara, S. K. Boopathi, N. Hadjichristidis, Y. Gnanou and X. Feng, *Macromolecules*, 2021, **54**, 2711–2719.
44 Z. Chen, J.-L. Yang, X.-Y. Lu, L.-F. Hu, X.-H. Cao, G.-P. Wu and X.-H. Zhang, *Polym. Chem.*, 2019, **10**, 3621–3628.
45 A. Kummari, S. Pappuru and D. Chakraborty, *Polym. Chem.*, 2018, **9**, 4052–4062.
46 K. A. Andrea and F. M. Kerton, *ACS Catal.*, 2019, **9**, 1799–1809.
47 K. Andrea and F. Kerton, *RSC Adv.*, 2019, **9**, 26542–26546.
48 K. A. Andrea, M. D. Wheeler and F. M. Kerton, *Chem. Commun.*, 2021, **57**, 7320–7322.
49 J. Coudane, H. Van Den Berghe, P. Gonzalez, J. Mouton, B. Nottelet and X. Garric, *Polym. Rev.*, 2026, 1–24.
50 Y. Yu, M. Kim, G. S. Lee, H. W. Lee, J. G. Kim and B.-S. Kim, *Macromolecules*, 2021, **54**, 10903–10913.
51 H. Liu, V. A. Maugein and D. M. Haddleton, *Polym. Chem.*, 2024, **15**, 2862–2872.
52 G. Le Fer, J. Babinot, D.-L. Versace, V. Langlois and E. Renard, *Macromol. Rapid Commun.*, 2012, **33**, 2041–2045.
53 C. O. Kappe, *Chem. Soc. Rev.*, 2008, **37**, 1127–1139.
54 M. J. Sanford, L. Peña Carrodeguas, N. J. Van Zee, A. W. Kleij and G. W. Coates, *Macromolecules*, 2016, **49**, 6394–6400.
55 F. P. Byrne, S. Jin, G. Paggiola, T. H. M. Petchey, J. H. Clark, T. J. Farmer, A. J. Hunt, C. R. McElroy and J. Sherwood, *Sustainable Chem. Processes*, 2016, **4**, 7.
56 L. J. Diorazio, D. R. J. Hose and N. K. Adlington, *Org. Process Res. Dev.*, 2016, **20**, 760–773.
57 F. C. Schilling and A. E. Tonelli, *Macromolecules*, 1986, **19**, 1337–1343.
58 M. I. Childers, J. M. Longo, N. J. Van Zee, A. M. LaPointe and G. W. Coates, *Chem. Rev.*, 2014, **114**, 8129–8152.
59 M. S. Young, A. M. LaPointe, S. N. MacMillan and G. W. Coates, *J. Am. Chem. Soc.*, 2024, **146**, 18032–18040.
60 A. Sirin-Sariaslan and S. Naumann, *Chem. Sci.*, 2022, **13**, 10939–10943.
61 A. Sirin-Sariaslan and S. Naumann, *Chem. Commun.*, 2023, **59**, 11069–11072.
62 Y.-B. Fang, H. Qi, B. Li, G.-W. Yang and G.-P. Wu, *Polym. Chem.*, 2024, **15**, 1297–1302.
63 G. Yang, Y. Zhang, R. Xie and G. Wu, *J. Am. Chem. Soc.*, 2020, **142**, 12245–12255.
64 D. Some WP1615: *SEC-MALS for absolute biophysical characterization*, Wyatt Technology LLC, 2024.
65 W. Gao and M. Chen, *AN1002: Characterizing the Average Composition and Molar Mass Distributions of a Copolymer by SEC-MALS-dRI-UV*, Wyatt Technology LLC, 2019.
66 S. Koltzenburg, M. Maskos and O. Nuyken, *Polymer chemistry*, Springer, Berlin [Heidelberg], 2nd edn, 2023.
67 J. D. Menczel and R. B. Prime, *Thermal analysis of polymers: fundamentals and applications*, John Wiley, Hoboken, N.J, 2009.

68 M. Baer, *J. Polym. Sci., Part A: Gen. Pap.*, 1964, **2**, 417–436.
69 C. Koning, J. Wildeson, R. Parton, B. Plum, P. Steeman and D. J. Darensbourg, *Polymer*, 2001, **42**, 3995–4004.
70 M. Hassan, G. A. Bhat and D. J. Darensbourg, *Polym. Chem.*, 2024, **15**, 1803–1820.
71 M. Sengoden, V. Satheesh, S. Sarkar and D. J. Darensbourg, *Polym. Chem.*, 2025, **16**, 4548–4556.
72 M. J. Sanford, N. J. V. Zee and G. W. Coates, *Chem. Sci.*, 2017, **9**, 134–142.
73 *JASPER - JavaScript Percentage Elemental Calculator v2.0. PGP*, https://www.yorku.ca/pgpotvin/public/Jasper/jasper2.htm, (accessed January 21, 2026).
74 R. E. H. Kuveke, L. Barwise, Y. Van Ingen, K. Vashisth, N. Roberts, S. S. Chitnis, J. L. Dutton, C. D. Martin and R. L. Melen, *ACS Cent. Sci.*, 2022, **8**, 855–863.
75 A. Nogalska, A. Trojanowska, B. Tylkowski and R. Garcia-Valls, *Phys. Sci. Rev.*, 2020, **5**, 20190083.
76 S. D. Thorat, P. J. Phillips, V. Semenov and A. Gakh, *J. Appl. Polym. Sci.*, 2003, **89**, 1163–1176.